Supplementary Information

Dimension-shifting multifunctional biocompatible nanocomposites

Weiquan Chen,[a] Xiaozhu Chen,[a] Yongshi Liang,[a] Jianfeng Lai,[a] Liye Xia,[a] Lu Wen*[b] and Gang Chen*[a]

a. School of Pharmacy, Guangdong Pharmaceutical University, Guangzhou, 510006, China
Guangdong Provincial Key Laboratory of Advanced Drug Delivery, Guangdong Pharmaceutical University, Guangzhou, 510006, China
Guangdong Provincial Engineering Center of Topical Precise Drug Delivery System, Guangdong Pharmaceutical University, , Guangzhou, 510006, China
b. School of Pharmacy, Guangdong Pharmaceutical University, Guangzhou, 510006, China

Materials. N, O-carboxymethyl chitosan (Mw: 90 kDa, degree of deacetylation: 80.1%) was purchased from AK BIOTECH LTD. (Shandong, China). Chitosan (Mw: 5 kDa, degree of deacetylation: 80%-85%) and Chitosan (Mw: 300 kDa, degree of deacetylation: 80%-85%) was purchased from Yuhuan Ocean Biochemical Co. (Zhejiang, China). Calcium chloride was purchased from Tianjin Guangcheng Chemical Co. Ltd. (Tianjin, China). Sodium carbonate was purchased from Tianjin Damao Chemical Co. Ltd. (Tianjin, China).Iron (Ⅱ, Ⅲ) oxide (Fe_3O_4, 99.5%, MW= 231.53) was obtained from Shanghai Puzhen Biotechnology Co. Ltd. Poly lactic-co-glycolic acid (LA: GA=75:25, Mw ~15000) was purchased from Shandong Medical Instrument Research Institute (Shandong, China). Polyvinyl alcohol 4-88(PVA, Mw~31000) was purchased from Sigma-Aldrich (USA). Perfluoro-15-crown-5-ether (PFC, 99%, MW= 580.08) was obtained from J&K Scientific Ltd. H_2O_2 and sodium carbonate were purchased from Guangzhou Chemical Reagent

Factory (Guangzhou, China). Dichloromethane was purchased from Tianjin Fuyu Chemical Co. Ltd. (Tianjin, China). Tween 20, and ethanol were purchased from Tianjin Yongda Chemical Co. Ltd. (Tianjin, China). γ-poly-glutamic acid (γ-PGA) was purchased from Shenzhen Simeiquan Biotechnology Co. Ltd. (Shenzhen, China). Distilled water was supplied by Guangzhou Watson's Food & Drinks Co. Ltd. (Guangzhou, China). Nile red (NR) was purchased from Guangzhou Qiyun Biotechnology Co. Ltd. (Guangzhou, China). Coumarin-6 (C-6) was purchased from Sigma-Aldrich (USA). D-(+)-gluconic acid δ-lactone(GDL; ≥99.0%) was purchased from Aladdin. Hoechst 33342 and Propidium Iodide (PI) were purchased from Sigma-Aldrich (USA). All other chemicals were of reagent grade and were used without any purification.

Preparation of CS-PLGA NPs. CS-PLGA NPs containing PFC and Fe_3O_4 with or without Coumarin-6 dye were prepared using a double emulsion (water/oil/water) solvent evaporation process. Briefly, PFC solution (250 μL) and Fe_3O_4 nanoparticles(30 mg) were added to PLGA (30 mg) dissolved in dichloromethane (1 mL), into which CS-PVA solution（8 ml, chitosan-acetic acid solution (Mw: 300 kDa) was dissolved in 5% wt/vol PVA solution) was then added. After being well blended, the mixture was sonicated using a sonifier equipped with microtip in an ice water bath for 2 min in total, with 5-second-on, 5-second-off, 30% power output. Then another 11 mL PVA solution was added to homogenize the emulsion, which was stirred later for 4 hours in open at room temperature to vaporize organic solvents. The product was then centrifuged at 15000 rpm for 30 min, and washed 5 times with purified water to remove excessive PVA and CS. The final charged nanoparticles powder of CS-PLGA NPs or CS-PLGA(C-6) NPs were collected and obtained by lyophilization for 2 days.

Preparation of CMCS/CC-CS NPs. CMCS/CC-CS NPs containing Fe_3O_4 with or without Nile Red dye were prepared using an ion exchange method process. Briefly, 42 mg of CMCS was dissolved in 20 mL of deionized water at room temperature, then 2 mL of Na_2CO_3 (0.02 M) was added and stirred for 0.5 h. Thereafter, 2 mL of $CaCl_2$ (0.02 M) was added to the mixtures dropwise and stirred for 1 h. The precipitate was centrifugated, washed with water several times, and dried in an oven to obtain CMCS/CC NPs. The CMCS/CC NPs loaded with Nile red was prepared as follows: Nile red (1 mg) was dissolved in Tween 80 (0.6 mL) and then was mixed with Na_2CO_3 solution. Then the follow-up methods were the same as the preparation of blank CMCS/CC NPs.

An amount of 30 mg of nano- Fe_3O_4 was dissolved in 10 mL, 5 mg/mL of CS solution (Mw: 5 kDa) by an ultrasonic disperse method. And then the suspension was added to 20 mL 40 mg/mL CMCS/CC NPs. After stirred for 30 min, 2 mL γ-PGA (7.5mg/mL) solution was added to this suspension. After 30 min of mechanical stirring (800 rpm), the particles were centrifuged at 4000 rpm for 10 min and then added to 5 mL 0.5 mg/mL $FeCl_3$ solution for 3 h. The products were purified by centrifugation at 3,000 rpm for 10 minutes, and further purified by dialysis method. The supernatants were decanted and analyzed after freezedrying. The preparation of CMCS/CC-CS NPs loaded with Nile red was the same as that of CMCS/CC NPs loaded with Nile red. The product was then centrifuged at 15000 rpm for 30 min, and washed 5 times with purified water to remove NaCl. The final charged nanoparticles powder of CMCS/CC-CS NPs or CMCS/CC-CS (NR) NPs were collected and obtained by lyophilization for 2 days.

Preparation of one-dimensional CS-PLGA@CMCS/CC-CS composite nanochains. The composite nanochains with different weight ratios of CS-PLGA NPs to CMCS/CC-CS NPs (R) were dispersed in purified water with adjusted pH = 8 (using NaOH), respectively. After shaking, the samples were added onto the silicon wafers under an ultra-low magnetic field (5 mT) at room temperature. The external magnetic field would induce the CS-PLGA and CMCS/CC-CS composite nanoparticles to arrange linearly along the direction of the external magnetic field. After the solvent was dried out, the linear assemblies of CS-PLGA@CMCS/CC-CS composite nanochains were observed by scanning electron microscopy (SEM). Meanwhile, the samples with different R were added onto the glass slides at 5 mT to observe the assembly process by optical microscope and confocal laser scanning microscope (CLSM). The excitation and emission wavelengths described below were used: Nile red: excitation at 543 nm, emission at 600–670 nm; C-6: excitation at 488 nm, emission at 493–538 nm.

Preparation of three-dimensional CS-PLGA@CMCS/CC-CS composite gels. CS-PLGA NPs and CMCS/CC-CS NPs suspensions of similar volume fraction were prepared that contained 20 mM of NaOH. Thereafter, depending on the required CS-PLGA -to- CMCS/CC-CS ratio R and total solids concentration (φ), specific volumes of the CMCS/CC-CS NPs suspension were added to the CS-PLGA NPs suspension and mixed by vortexing. To initiate gel formation, 50mM of GDL powder was added to the mixed suspension at pH~11.

pH measurements. The pH measurements were performed using a pH meter (PHS 25, Shanghai Yidian Scientific Instrument Co., Ltd.). For the real-time measurements of pH of mixed dispersions as a function of the decomposition time of GDL, 5 mL of dispersion was used and the GDL powder (80mM) was added just before the measurement.

Particle size and Zeta potential measurements. The size of swollen nanoparticles in water was measured by Zetasizer (Nano S90, Malvern Instruments Ltd.)**.** The zeta potential of nanoparticles was measured using a Zetasizer (Beckman Coulter Commercial Enterprise Co. Ltd.) at 25 °C by dispersion of nanoparticles in purified water with adjusted pH (using HCl or NaOH). Each zeta potential value represents an average of three measurements which were calculated by the Beckman software based on the measured mobility of nanoparticles according to the Smoluchowski equation.

Release of Nile red in CMCS/CC NPs and CMCS/CC-CS NPs. An amount of 2 mL of H_2O_2 (200, 100 mM) was added to 2 mL of CMCS/CC NPs or CMCS/CC-CS NPs loaded with Nile red, after adjusted the pH value of the solutions to 5.0, 6.0, and 7.4 with PBS, the solutions were incubated at 37°C. At various time points, the solutions were collected, and the Nile red level was determined by a fluorospectrophotometer (RF-5301PC, Shimadzu Corp., Kyoto, Japan).

Measuring the oxygen carrying ability. Then we measured the oxygen carrying ability of CS-PLGA NPs following Song's report.[1] Firstly, 2 mL of as-prepared CS-PLGA NPs solution stored in a 50 mL sample tube was diluted to 6 mL with deionized water, and then placed in an asepticoxygen chamber (O_2 flow rate= 5 L/min) for 20 s for oxygenation. Afterwards, the oxygen concentrations in aqueous solutions (4 mL) were measured with a portable dissolved oxygen meter (Rex, JPBJ-608, China) before and after adding 2 mL CS-PLGA NPs solution. In addition, CS-PLGA NPs solution without oxygenation, CS-PLGA NPs solution with oxygenation, H_2O with oxygenation, H_2O without oxygenation, and PFC with oxygenation were treated as control groups.

Rheological experiments. Rheological experiments were performed using an Advanced Rheology Expanded Systems (TAARES/RFS, TA Instrument Ltd.). 2° cone steel plates (20 mm diameter) were used and the 500-um gap was filled with tested colloidal gel. A solvent trap was used to prevent evaporation of water. The storage modulus (G') of the sample were determined at 20℃ by forward and-backward stress sweep experiments. The shear-thinning behavior of

the gels was determined by measuring their viscosity while varying the shear rate from 0 to 200 s^{-1}.

Cell culture. Mouse fibroblast cells L929 were provided by Type Culture Collection of the Chinese Academy of Sciences (Shanghai, China) and were seeded at a density of 1×10^4 cells per cm^2. Cells were grown to near confluence in the individual wells of a 24-well tissue culture-treated plate and then exposed to colloidal gel. Cells were cultured on the colloidal gels for 24h and 72h, the media being carefully changed every two to three days without disturbing the settled gels at the bottom. Subsequently, the cells were stained with Hoechst 33342 /PI reagent (red-fluorescent dye for dead cells and blue-fluorescent dye for all cells) and incubated for 10 min, before being subjected to fluorescence microscopy.

Cytotoxicity. L929 cells were incubated with CS-PLGA NPs, CMCS/CC-CS NPs, CS-PLGA@CMCS/CC-CS nanochains and CS-PLGA@CMCS/CC-CS gels at different density each for 24 h in a humidified incubator at fully humidified atmosphere at 37 °C, 5% CO_2 and 95% room air, respectively. The cytotoxic effects of nanoparticles, nanochains and colloidal gels on L929 were determined by MTT colorimetric assay, respectively.

Other characterization. Transmission electron microscopy (TEM, H-7650 HITACHI) images of CS-PLGA NPs and CS-PLGA@CMCS/CC-CS gels. Scanning electron microscopy (SEM) was performed using a Zeiss Gemini500 field emission scanning electron microscope. The physical form (crystalline or amorphous) of the CMCS, $CaCO_3$ and CMCS/CC NPs were obtained using an X-ray diffractometer (Bruker Smart 1000 CCD, Bruker Corporation, Billerica, MA, USA). The scanning speed was 2°/min, and scanning angles ranged from 5° to 80°. The structural characteristics of the Series CS-PLGA NPs and Series CMCS/CC-CS NPs were detected using Fourier transform infrared spectroscopy (FTIR) (Spectrum 100, PerkinElmer Inc., Waltham, MA, USA) and recorded in KBr pellets with four scans at a resolution of 4 cm^{-1} over a wave number range of 4000-450 cm^{-1}. In addition, thermo gravimetric analysis (TGA, TG209F1 libra) and Magnetic Property Measurement System (VSM, MPMS XL-7, Quantum Design, USA) measurements were carried out.

Statistics. Significant differences between groups were determined through analysis of variance, multiple comparison test and independent-samples t-test with SPSS 19.0 software (Chicago, IL, USA). $P < 0.05$ was considered statistically

significant.

The principle of Brownian motion led to the statistical arrangement. Each nanoparticles could be approximated as a pointdipole with a magnetic moment under an external magnetic field, which was determined by the amount of superparamagnetic Fe_3O_4 nanoparticles encapsulated within the composite nanoparticles. As shown in Figure 6c, when a unidirectional magnetic field of magnitude H_0 was applied, the field induces a magnetic dipolar moment in the magnetic particles m: [2]

$$m = 4\pi a^3 \vec{H}_0(\mu_P + \mu_S) \,/\, (\mu_P + 2\mu_S) \quad (1)$$

where a is the radius of the nanocomposites and μ_p and μ_s are the permeability of the particles and the solvent, respectively.

The responsible force to induce linear arrangement of the composite nanocomposites is given by[3]

$$F = -\frac{3\mu_0}{4\pi r^4}\left(3\left(\vec{m}_1 \cdot \vec{r}_0\right)\left(\vec{m}_2 \cdot \vec{r}_0\right) - \vec{m}_1 \cdot \vec{m}_2\right) \quad (2)$$

where r is the distance between the centers of the two dipoles;r_0 is the the unit vector in the r direction, $\vec{m}_1$ and $\vec{m}_2$ are the magnetic moments of two nanoparticles respectively; μ_0 is the magnetic permeability of a vacuum.

More importantly, a key dimensionless parameter to characterize the formation of chains is the ratio between the magnetic and thermal energies [4] :

$$\alpha = m^2/\left(8a^3 K_b T\right) \quad (3)$$

where K_b is the Boltzmann constant, and T is the temperature. Herein the ultra-low magnetic field (5 mT) was used to study the reversible morphologies between linear assemblies and assembly units at room temperature. The obtained α was large enough so that the magnetic interactions would dominate over Brownian thermal motion[4]. Under the external magnetic field, the large magnetic moments enabled the attractive and repulsive dipolar interactions between the composite nanoparticles to overcome thermal motion. As a result, the composite nanoparticles would migrate and arrange linearly along the magnetic line of force as well as spatially stagger with adjacent composite nanoparticles so as to minimize the local magnetostatic energy (Fig. S3). With the increase of the magnetic field, the saturation magnetization values of the composite nanoparticles increased gradually. The composite nanoparticles carried a lager net magnetic dipole moment (m), contributing to better migration and arrangement of the composite

nanoparticles. As a result, the linear trends of the assemblies turned to be more obvious. After the magnetic field adjusted to the appropriate value, the composite nanoparticles could acquire relatively appropriate driving force for better assembly, resulting that the assemblies showed an excellent linear aligned arrays.

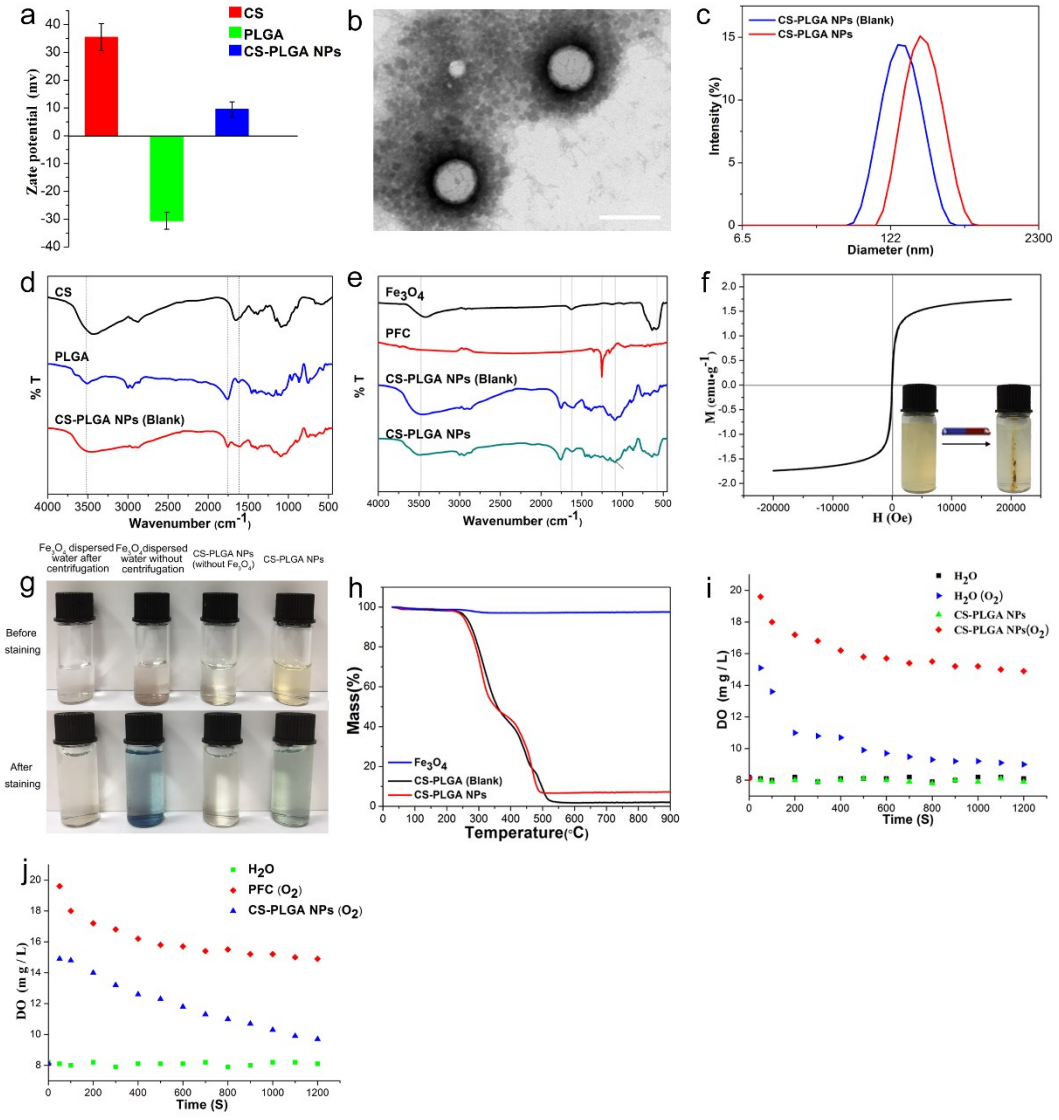

Figure S1. (a) Zeta potentials of CS, PLGA and CS-PLGA NPs. (b) TEM image of CS-PLGA NPs. Scale bar: 200 nm. (c) Size distribution pattern of the CS-PLGA NPs and CS-PLGA NPs Blank (without Fe_3O_4 and PFC). (d) FTIR characterization of CS, PLGA and CS-PLGA emulsion(without PFC and Fe_3O_4). (e) FTIR characterization of Fe_3O_4, PFC, CS-PLGA NPs and CS-PLGA NPs (Blank). (f) Magnetic hysteresis loop for CS-PLGA NPs at room temperature. (g) Prussian blue dye digital image of CS-PLGA NPs. (h) TGA of Fe_3O_4, CS-PLGA NPs and CS-PLGA NPs (Blank). (i) The measurement of oxygen

concentrations in water after adding PFC or CS-PLGA NPs with oxygen pre-saturation. (j) Oxygen concentrations over time in water after adding CS-PLGA NPs with or without presaturation with oxygen. In this experiment, the same volume of oxygen-saturated water was spiked into a large volume of deionized water as the control (blue triangle).

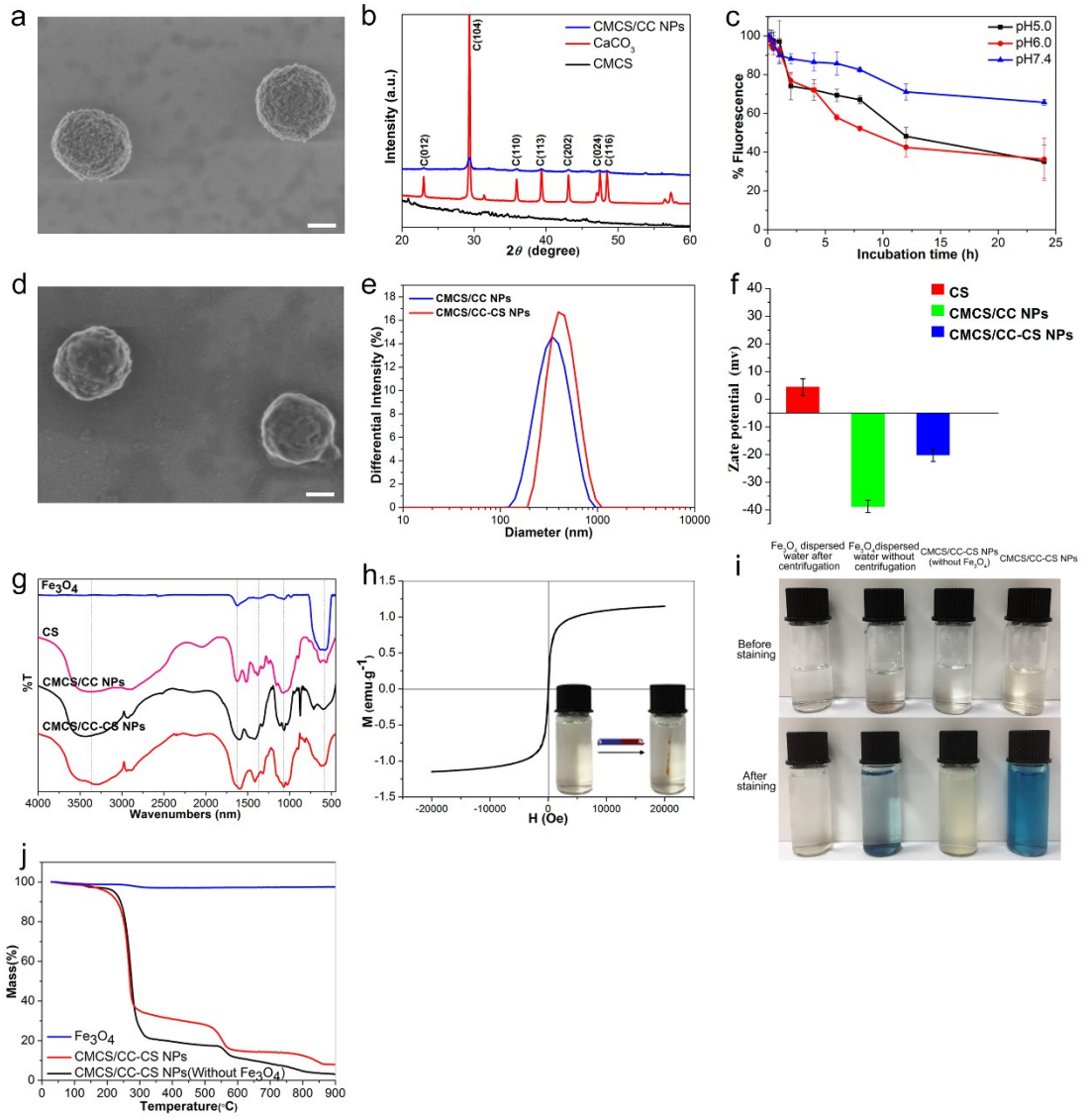

Figure S2. (a) SEM micrographs of CMCS/CC NPs. (b) XRD pattern of CMCS/CC NPs. (c) The release profiles of CMCS/CC NPs encapsulating NR at different pH conditions. (d) SEM micrographs of CMCS/CC-CS NPs. (e) Size distribution of CMCS/CC NPs and CMCS/CC-CS NPs. (f) Zeta potentials of CS, CMCS/CC NPs and CMCS/CC-CS NPs. (g) FTIR spectra of CMCS/CC NPs and CMCS/CC-CS NPs. (h) Magnetic hysteresis loop for CMCS/CC-CS NPs at room temperature. (i) Prussian blue dye digital image of CMCS/CC-CS NPs. (j) TGA of Fe_3O_4, CMCS/CC-CS NPs (without

Fe_3O_4) and CMCS/CC-CS NPs. Scale bar: 200 nm.

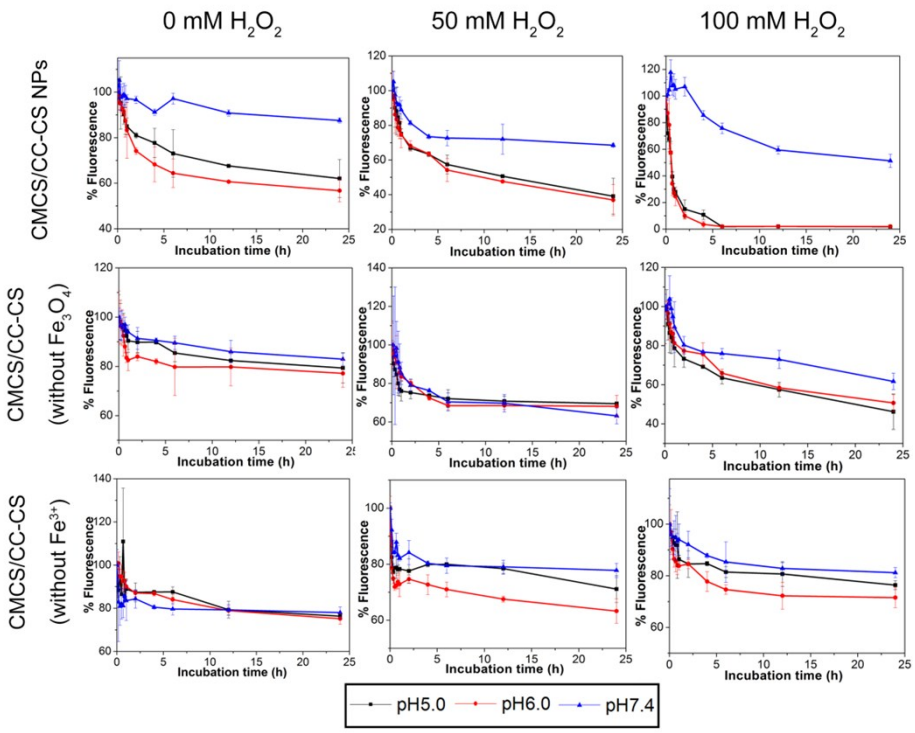

Figure S3. The release profiles of CMCS/CC-CS NPs in the absence or presence of various concentration gradients of H_2O_2 and pH.

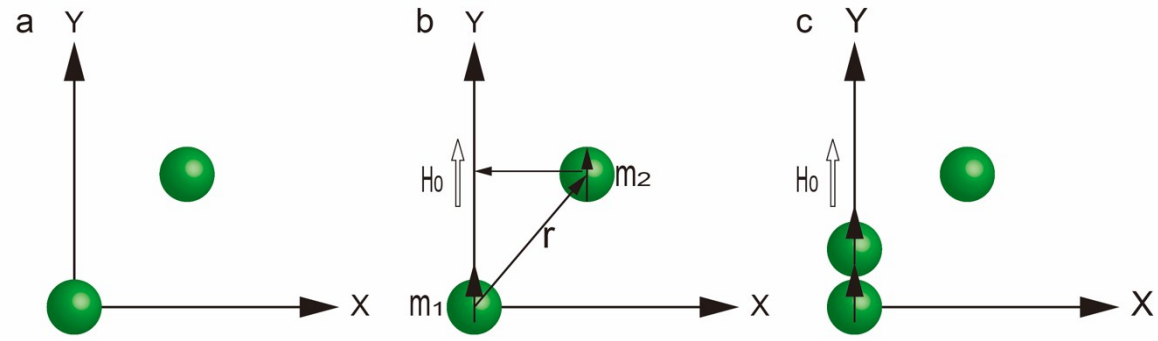

Figure S4. Schematic of migrating to linear arrangement of the composite nanospheres. (a) without an external magnetic field; (b and c) under an external magnetic field.

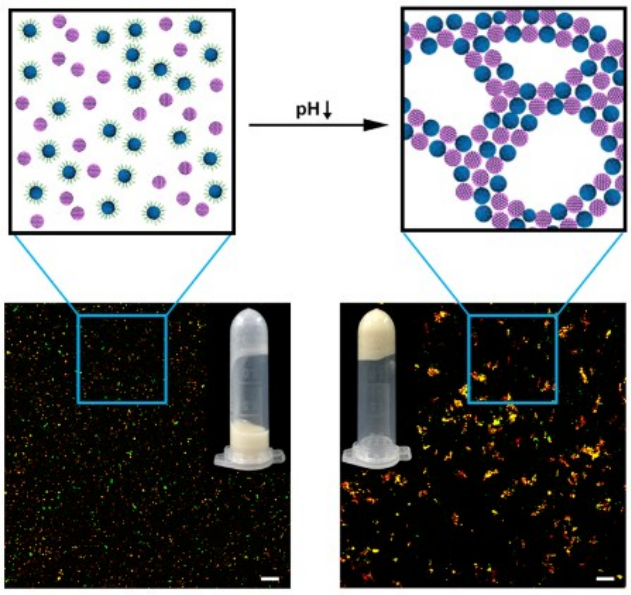

Figure S5. Schematic illustration of the 3D gel formation. The gel structure was visualized by confocal microscope (both before and after gel formation). Green and red particles represent CS-PLGA NPs and CMCS/CC-CS NPs, respectively. Scale bar: 50 µm.

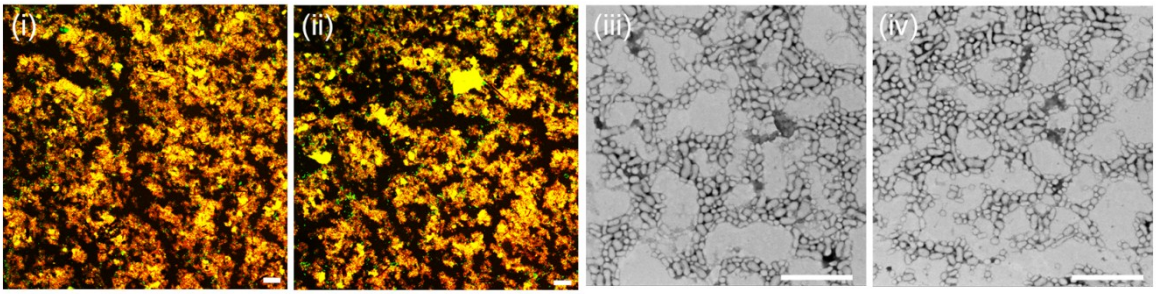

Figure S6. Confocal images of a colloidal gel with R=5 and φ=5 % wt/vol (i) before and (ii) after addition of an excessive amount 100mM NaOH solution. Scale bars represent 50 µm. TEM images of colloidal gel with R=5:5 and φ=5 % wt/vol (iii) before and (iv) after addition of an excessive amount 100mM NaOH solution.

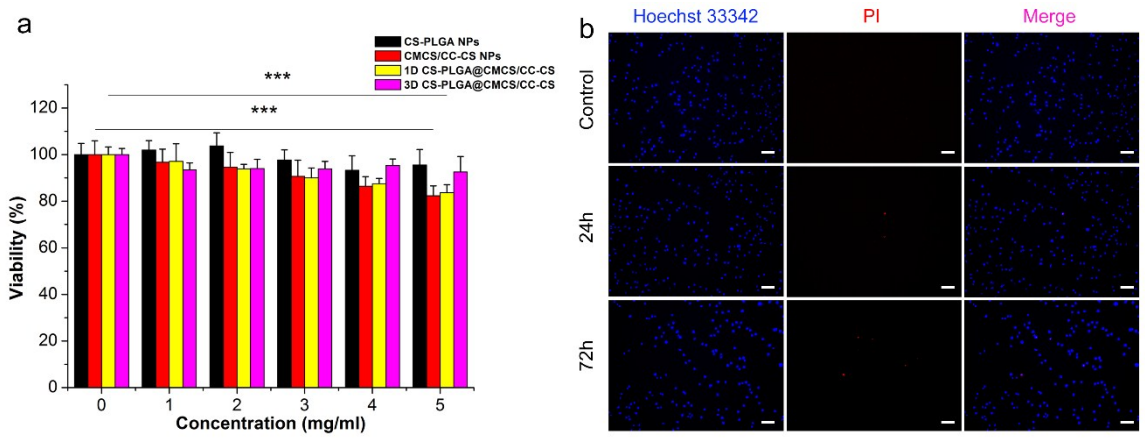

Figure S7. (a) Cell viability of L929 cells incubated with three kinds dimensional nanocomposites for 24 h. *P < 0.05, **P <0.01, ***P <0.001 vs. control group. Results were shown as mean ± SD (n=6). (b) LIVE/DEAD assay of L929 cells after 24 and 72 h of 3D culture in the composite colloidal gels (R=5:5, φ=10% wt/vol). Scale bar: 100 μm.

Movie. S1.

File name: S1.mp4

Content: An optical microscopy movie showing the dimension-shifting of 0D and 1D nanocomposites by the change of magnetic field (R=5:5).

Movie. S2.

File name: S2.mp4

Content: The shape recovery of nanogels with R=5:5 and φ=5 % wt/vol.

References

1 X. Song, L. Feng, C. Liang, K. Yang and Z. Liu, *NANO LETT*, 2016, **16**, 6145-6153.
2 J. T. B, *In Electromechanics of particles*, New York: Cambridge University Press, 1995, pp. 125-135.
3 R. Tao, *Journal of Physics: Condensed Matter*, 2001, **13**, R979-R999.
4 S. Melle, G. G. Fuller and M. A. Rubio, *PHYS REV E*, 2000, **61**, 4111-4117.